

Thin Film Transformer and Its Analysis by Integral Equation Method

I. Marinova, Y. Midorikawa, S. Hayano, and Y. Saito

Abstract—Recently, we proposed a new high frequency transformer that could allow the manufacture of small power supplies. In this paper, we propose a thin film transformer for small electronic devices, and apply the integral equation method to analyze this transformer. Both the primary and secondary coils of the film transformer are arranged coaxially on one layer and multiply laminated. The operation principal of the transformer is based on the skin effect and the mutual effect between the coils at high frequency. Because of the coaxially arranged coils, the magnetic field of the transformer can be modeled with an axisymmetric assumption. Using the model, we evaluate the electromagnetic field and calculate the lumped circuit parameters, i.e., inductance and resistance, which are compared with experimental values. A fairly good agreement is obtained. Thus, the applied method is quite useful for design and investigation of the thin film transformer.

I. INTRODUCTION

WITH the developments of modern electronic devices such as the notebook computer, word processor and cordless telephone, it is essential to reduce the size and weight of their electric power supplies. The key to designing compact electric power supplies is to reduce the size of the magnetic devices, e.g., reactors and transformers. One of the ways to reduce the size of a magnetic device is to employ high frequency excitation [1], [2]. In such high frequency operation, a serious problem is that the performance of the device is dominated by the frequency characteristics of the core magnetic materials. To overcome this difficulty, new magnetic materials typically represented by amorphous magnetic materials have been used [3], [4]. Nevertheless, it is difficult to avoid an essential increase of iron loss in accordance with the rise of operating frequency. Another solution of this problem is to exploit a coreless transformer. Already, we have succeeded in making a coreless transformer with high efficiency and demonstrated its usefulness for the dc to dc converters [5].

In this paper, a thin and light weight high frequency transformer which we call a film transformer is proposed. This new transformer is composed of the lamination of thin film conductors. Each film is constructed by the chemical etching processes. The operating principal is

based on the skin effect similar to that of our coreless transformer [5]. This fact was confirmed by comparing their frequency characteristics. To design and improve the film transformer characteristics, it is essential to analyze its electromagnetic phenomena and parameters. Both the primary and secondary coils of our film transformer are arranged coaxially on the one layer and multiply laminated. Because of these coaxially arranged coils, the magnetic field of the transformer can be modeled with an axisymmetric assumption. Since the operation principal of the transformer is based on the skin effect, the development of a computational model that takes into account the skin effect is extremely important. Applying the numerical methods, e.g. the finite element method (FEM) and boundary element method (BEM) to this problem leads to results with good accuracy. Particularly, some calculation methods for voltage-source problems that consider the current distributions in conductors are very useful tools for the design of magnetic devices [6]–[14]. These methods have been used to various voltage-source problems but have not always produced acceptably accurate solutions. In the present, we applied a method to obtain more exact current distributions in thin film conductors of the transformer. This method uses Fredholm integral equation of the second kind about the electric field intensity. It is quite convenient for the thin film transformer analysis, because the modeling for unbounded problems with homogeneous media is easy and accurate solutions can be obtained. To demonstrate the advantages of the method, using a vector potential expression, we calculate the magnetic field, impedance and ratio of transformation of the thin film transformer for various frequencies under the open and short secondary circuit conditions. The results obtained show good agreement with experimental results. Thus, the applied method is quite useful for design and investigation of the thin film transformer.

II. FILM TRANSFORMER

A. Geometry

Constructive shape and geometry of the thin film transformer are shown in Figs. 1 and 2. This transformer is composed of two layers primary and secondary coils. Connections between layers of separate coils are serial. Fig. 2 shows the sizes of the separate turns and the dis-

Manuscript received November 5, 1993; revised January 19, 1995.

I. Marinova is on leave from Technical University of Sofia, Department of Electrical Apparatus, Sofia-1156, Bulgaria.

Y. Midorikawa, S. Hayano, and Y. Saito are with the College of Engineering, Hosei University, Kajino Koganei, Tokyo 184, Japan.

IEEE Log Number 9410683.

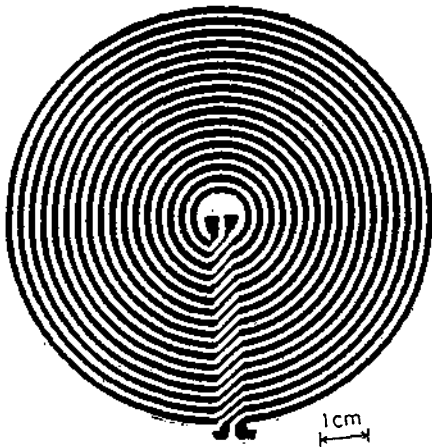


Fig. 1. Thin film transformer.

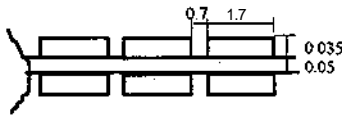


Fig. 2. The sizes of the turns (unit in mm).

tances between them. This transformer may be composed of two, four or more layers.

B. Method of Analysis

1) *Governing Equation for Eddy Current Problems:* If we assume the materials to be **homogeneous**, isotropic and neglect the displacement current, then the governing and constitutive equations in the eddy current region are given as follows

$$\text{rot} \mathbf{H} = \mathbf{J}_e \quad (1)$$

$$\text{rot} \mathbf{E} = -\frac{\partial \mathbf{B}}{\partial t} \quad (2)$$

$$\text{div} \mathbf{B} = 0 \quad (3)$$

$$\text{div} \mathbf{E} = 0 \quad (4)$$

$$\mathbf{B} = \mu \mathbf{H} \quad (5)$$

$$\mathbf{J}_e = \sigma \mathbf{E}, \quad (6)$$

where \mathbf{H} , \mathbf{J}_e , \mathbf{E} , \mathbf{B} , μ , σ are the magnetic field intensity, the exciting current density, the electric field intensity, the magnetic flux density, the magnetic permeability and the electric conductivity, respectively.

From the above equations in the sinusoidal steady-state, the electric field intensity \mathbf{E} satisfies by the **Helmholtz** equation

$$\nabla^2 \mathbf{E} - j\omega\mu\sigma \mathbf{E} = 0, \quad (7)$$

where ω is the angular frequency and $j = \sqrt{-1}$.

2) *Electromagnetic Field in Conductors:* Let us consider a conductor supplied with sinusoidal voltage u , with the angular frequency ω . This voltage excites alternating

current in the conductor and alternating magnetic field in its surrounding space. Accordingly Faraday's law, we have

$$u = iR + \frac{d\Phi}{dt}, \quad (8)$$

where R is the resistance of the conductor and Φ is the interlinkage magnetic flux.

Using conventional loop analysis, the conductor is considered to consist of single current loops with current Δi . The magnetic flux can be calculated from the magnetic vector potential

$$\Phi = \oint_L \mathbf{A} d\mathbf{l} \quad (9)$$

and $\Delta i R_1$ can be expressed with the electric field intensity

$$\Delta i R_1 = \oint_L \mathbf{E} d\mathbf{l}, \quad (10)$$

where L refers to the current path in each loop.

The vector potential at the point Q can be represented by current distribution in the conductor

$$\mathbf{A}(Q) = \frac{\mu_0}{4\pi} \int_V \frac{\mathbf{j}(M) E(M) dV_M}{r_{QM}}, \quad (11)$$

where M is the point of current integration in the conductor volume V .

If we substitute Eqs. (9)-(11) into Eq. (8), then the integral equation for the electric field intensity in the conductor becomes

$$u = \oint_L \mathbf{E} d\mathbf{l} + j\omega \frac{\mu_0}{4\pi} \oint_L \int_V \left[\frac{\mathbf{j}(M) E(M) dV_M}{r_{QM}} \right] d\mathbf{l}, \quad (12)$$

where it must be noted that the conductor is fed a sinusoidal alternating voltage u , also the medium is homogeneous and isotropic.

For an electromagnetic field where a two-dimensional **axisymmetrical** model is acceptable, the integral equation (12) essentially simplifies and becomes a **Fredholm** integral equation of the second kind [15].

3) *Integral Equation for Axisymmetrical Electromagnetic Field:* Fig. 3 shows a conductor with an **axisymmetric** electromagnetic field. The current path is a closed circle contour with length $2\pi\rho_Q$.

The vector potential A and the current density $\sigma \mathbf{E}$ only have components directed tangent to the current contour. Then equation (12) can be presented in a form

$$u = 2\pi\rho_Q \dot{E}(Q) + j\omega 2\pi\rho_Q \dot{A}(Q). \quad (13)$$

The vector potential A at the point Q of the **axisymmetric** electromagnetic field is defined by the expression

$$\dot{A}(Q) = \frac{\mu_0}{2\pi} \int_S \sigma(M) \dot{E}(M) \sqrt{\frac{\rho_M}{\rho_Q}} f(k) dS_M, \quad (14)$$

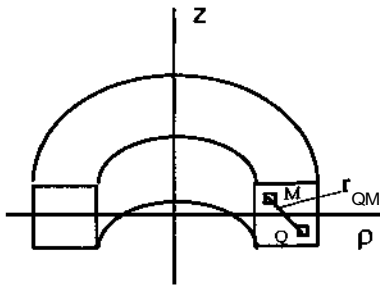


Fig. 3. A conductor with an axisymmetric electromagnetic field.

where S , Q and M are the cross-sectional area of the conductor, an observation point and a point of current integration, respectively. The function $f(k)$ is

$$f(k) = \frac{2}{\kappa} \frac{K(k) - E(k)}{k}, \quad (15)$$

where $K(k)$ and $E(k)$ are the complete elliptic integrals of the first and second kind with module k defined by the expression

$$k^2 = \frac{4\rho_Q\rho_M}{(\rho_Q + \rho_M)^2 + (z_Q - z_M)^2}. \quad (16)$$

Substituting Eqs. (14)–(16) into Eq. (13) yields the Fredholm integral equation of the second kind for the electric field intensity

$$\dot{E}(Q) + j\omega \frac{\mu_0}{2\pi} \int_S \sigma(M) \dot{E}(M) \sqrt{\frac{\rho_M}{\rho_Q}} f(k) dS_M = \frac{\dot{u}}{2\pi\rho_Q}. \quad (17)$$

This integral equation has a kernel with a weak logarithmic singularity. Solving (17), it is possible to determine the current distribution in the conductor due to the axisymmetric electromagnetic field. If the current distribution is known, then the different electromagnetic field characteristics are easily evaluated by means of the vector potential expression (14). For example, the impedance of the loop having a radius p , cross-section S and current I can be calculated from the electric field intensity and the vector potential using the expression

$$Z = \frac{2\pi}{IS} \int_S \rho(E + j\omega A) dS. \quad (18)$$

The inductance can be determined directly from

$$L = \frac{2\pi}{IS} \int_S \rho A dS. \quad (19)$$

4) *The System of Integral Equations:* When an electromagnetic system is composed of n parallel coaxial conductors and each conductor is fed by a voltage u_i , we con-

strain a system of integral equations

$$\begin{aligned} \dot{E}_i(Q) + j\lambda \sum_{i=1}^n \int_{S_i} \sigma_i(M) \dot{E}_i(M) \sqrt{\frac{\rho_M}{\rho_Q}} f(k) dS_i \\ = \frac{\dot{u}_i}{2\pi\rho_Q}, \quad i = 1, \dots, n \end{aligned} \quad (20)$$

where $X = \omega\mu_0/2\pi$ is the characteristic parameter of the integral equations.

The function u_i is constant over the conductor cross-section. The conductivity a is an integrand. Obviously, for inhomogeneous conductors, the conductivity may be a function of position. Integrating the system of equations (20) over the conductor section S_i , the system of integral equations for an electromagnetic system consisting of conductors with current excitation is as follows:

$$\begin{aligned} \dot{E}_i(Q) + j\lambda \sum_{i=1}^n \int_{S_i} \sigma_i \dot{E}_i(M) \sqrt{\frac{\rho_M}{\rho_Q}} \left[f(k) - \frac{1}{2\pi a_i \sqrt{\rho_Q}} \right. \\ \left. \cdot \int_{S_i} \sigma_i \frac{f(k)}{\sqrt{\rho_Q}} dS_i \right] dS_i = -\frac{\dot{I}_i}{2\pi\rho_Q a_i}, \end{aligned} \quad (21)$$

where $a_i = \int_{S_i} \frac{\sigma_i}{2\pi\rho_Q} dS_i$ and $i = 1, \dots, n$.

Thus, the electromagnetic field calculation of such electromagnetic system is reduced to a set of Fredholm integral equations of the second kind while the system is excited by the constant voltage or the current source.

5) *Numerical Aspects:* The system of integral equations (20) is numerically solved. After the discretization of the conductors and the evaluation of the surface integrals, a system of linear algebraic equations (SLAE) of high order is formulated. The SLAE can be expressed in the matrix-vector form

$$[\dot{C}] \cdot [\dot{E}] = [\dot{F}], \quad (22)$$

where $[\dot{C}]$, $[\dot{E}]$, $[\dot{F}]$ are the coefficient matrix, the vector of the unknown electric field intensity and the vector of the right side of the SLAE, respectively. After obtaining the inverse matrix $[\dot{C}]^{-1}$, which is an asymmetric-full matrix, the solution vector is given by

$$[\dot{E}] = [\dot{C}]^{-1}[\dot{F}]. \quad (23)$$

A computer program has been developed to realize the analysis method and to investigate the characteristics of the thin film transformer.

6) *Results and Discussion:* The method and computer program, presented above, are applied to the analysis of the thin film transformer.

Figs. 4 and 5 show the calculated results of the inductance and the resistance together with those of experiments for the various frequencies. By considering the re-

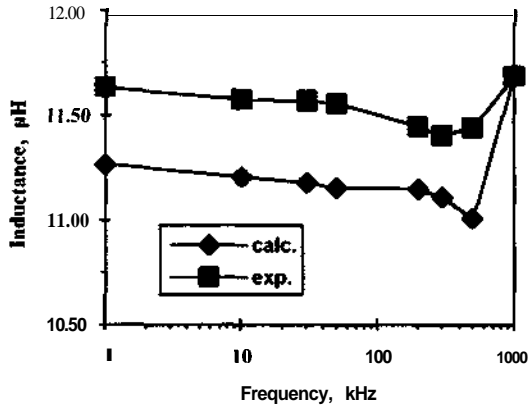


Fig. 4. Coil inductance vs. Frequency (two layer film transformer).

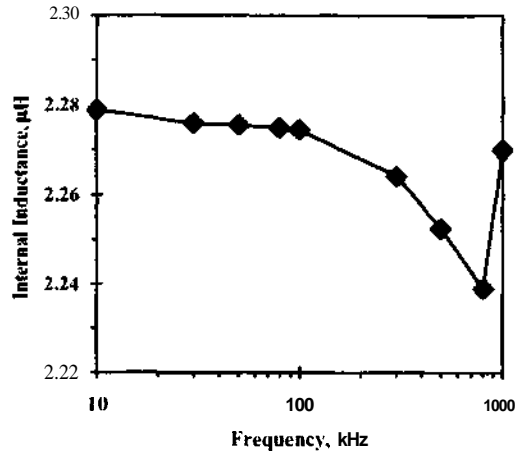


Fig. 6. Internal inductance vs. Frequency (two layer film transformer).

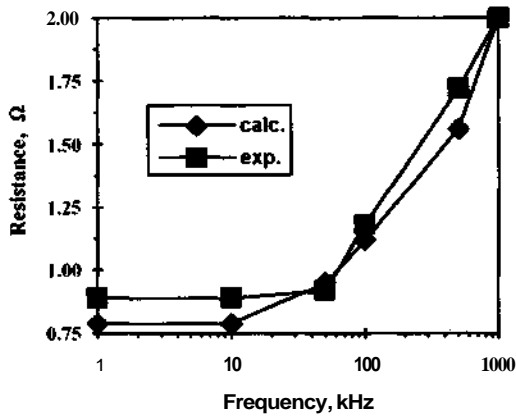


Fig. 5. Coil resistance vs. Frequency (two layer film transformer).

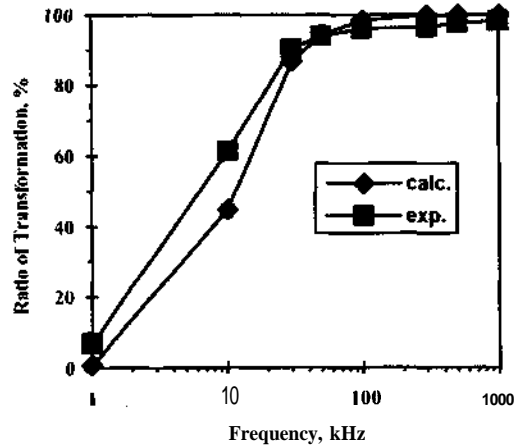


Fig. 7. Ratio of transformation vs. Frequency (two layer film transformer).

suits in Figs. 4 and 5, it is obvious that the coil's inductance decreases and the resistance increases due to the skin effect when the exciting frequency is raised up. The change of the inductance is approximately 7% and the change for the resistance is 50%. The inductance and the resistance increase significantly near the 1 MHz. Fig. 6 shows the calculated results concerning the change of the internal inductance as a function of frequency. Because of the skin effect, it decreases when the frequency increases and it begins to increase near 1 MHz. The phenomenon occurred near 1 MHz may be due to an edge effect of the films which, in turn, causes a significant change of the magnetic field distribution (see Fig. 9(c)). The results obtained from calculations coincide well with experiments. The difference between them is always less than 3.5% for the inductance and 10% for the resistance.

Fig. 7 shows the calculated ratio of transformation together with the experimental one. Clearly, when the frequency is increased, the induced voltage in the secondary coil simultaneously increases. After 50 kHz, the ratio of transformation exceeds 90%. Again the calculated values agree well with the measured values.

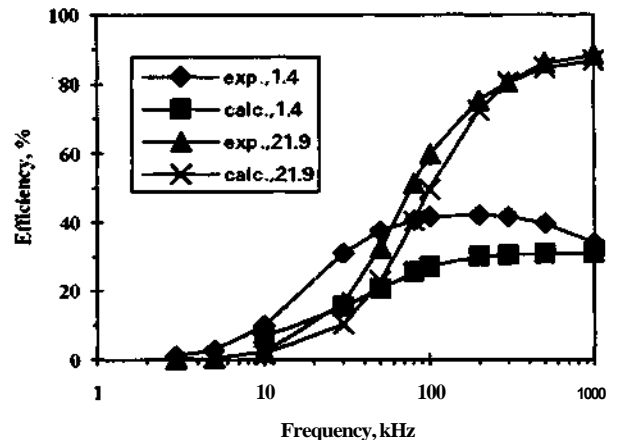


Fig. 8. Efficiency vs. Frequency Resistive load $R_2 = 1.4\Omega$ and $R_2 = 21.9\Omega$ (two layer film transformer).

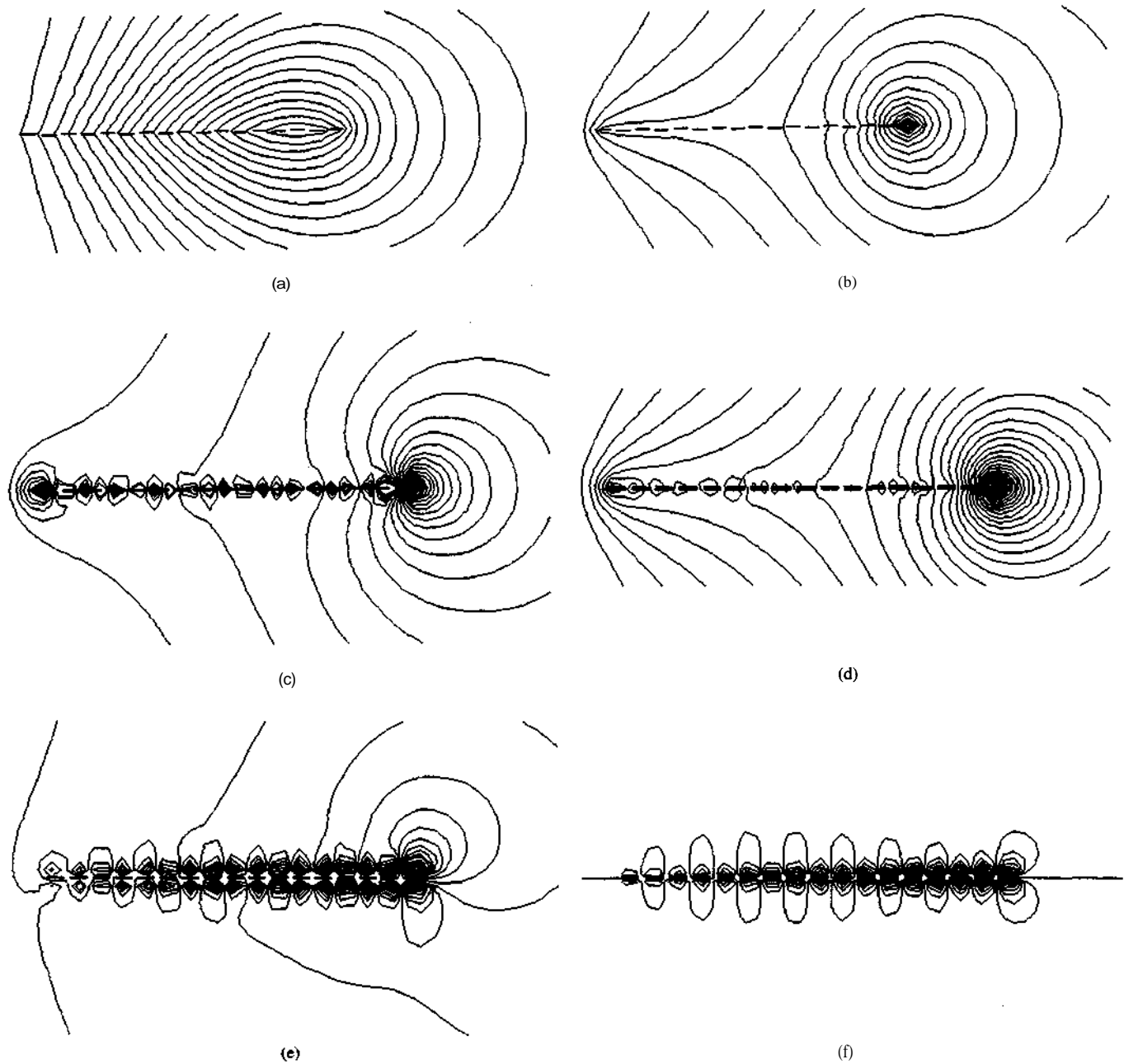


Fig. 9. Plot of the flux lines. (a) Two layer film transformer with open secondary circuit at 1 kHz frequency. (b) Two layer film transformer with open secondary circuit at 100 kHz frequency. (c) Two layer film transformer with open secondary circuit at 1 MHz frequency. (d) Four layer film transformer with open secondary circuit at 100 kHz frequency. (e) Two layer film transformer with short secondary circuit at 100 kHz frequency. (f) Four layer film transformer with short secondary circuit at 100 kHz frequency.

In Fig. 8 are shown the calculated and experimental results of the efficiency as a function of the frequency using two values of the pure resistive load $R_2 = 1.4\Omega$ and $R_2 = 21.9\Omega$ for a two layer film transformer. The efficiency exceeds 80% when the load is relatively bigger ($R_2 = 21.9\Omega$). This fact demonstrates the usefulness of the thin film transformer for constructing of the compact power supplies. The comparison of the computed results with those from measurements shows good agreement between them.

Figures 9(a)–(f) show the plots of the flux lines for two types of the film transformer at different frequencies under the secondary open and short circuited conditions. In Fig. 9(a) the applied frequency is 1 kHz, in Figs. 9(b), (d), (e), (f) – 100 kHz and in Fig. 9(c) – 1 MHz. Figs. 9(a)–(d) concern the modes with open secondary circuit, and Figs. 9(e), (f)—those with short secondary circuit. The results in Figs. 9(a)–(c) and (e) are for the two layer film transformer. Also, the results in Figs. 9(d) and (f) are for the four layer one. The magnetic field distribution is quite

different in the modes and the conditions, that are considered. The difference between the low and high frequencies is that the magnetic field is concentrated nearer to the coils in the high frequency case, especially when the transformer is composed of a large number of **layers**. The magnetic field distribution at 1 MHz frequency significantly changes because of the edge **effect** of the film transformer.

III. CONCLUSION

We have proposed a thin and lightweight high-frequency transformer and its analysis method based on the integral formulation. This film transformer demonstrates high efficiency and ratio of transformation. A method of analysis and computer program have been applied to investigation of the characteristics of thin film transformer. The results of the transformer analysis have correlated well with experimental results. Thus, it has been shown that the thin film transformer is significantly convenient for constructing of compact power supplies and the applied method for its analysis can be successively used to design such electromagnetic system composed of coaxial parallel conductors with a high-frequency voltage **supply**.

REFERENCES

- [1] K. Harada, T. Nabeshima, "Application of magnetic amplifier to high-frequency DC to DC converter," *Proc. IEEE*, vol. 76, April 1988, pp. 353-361.
- [2] F. C. Lee, "High-frequency quasi-resonant converter technology," *Proc. IEEE*, vol. 76, April 1988, pp. 377-390.
- [3] K. Arai, H. Tsutsumitake, and K. Ohmori, "Grain growth of rapid quenching high silicon-iron alloys," *IEEE Trans. Magn.*, vol. MAG-20, no. 5, pp. 1463-1465, Sept. 1984.
- [4] R. V. Major, T. M. Jasko, and K. J. Cruickshank, "Development of amorphous Fe-B based alloys for choke and inductor applications," *IEEE Trans. Magn.*, vol. MAG-20, no. 5, pp. 1415-1416, Sept. 1984.
- [5] S. Hayano, Y. Nakajima, H. Saotome and Y. Saito, "A new type high frequency transformer," *IEEE Trans. Magn.* vol. 27, no. 6, pp. 5205-5207, Nov. 1991.
- [6] M. J. Sablik, R. E. Beissner and A. Choy, "An alternative numerical approach for computing eddy currents: case of the double-layered

- plate," *IEEE Trans. Magn.*, vol. Mag-20, no. 3, pp. 500-506, May 1984.
- [7] J. H. McWhirter, R. J. Duffin, P. J. Brehm, and J. J. Oravec, "Computational methods for solving static field and eddy current problems via Fredholm integral equations," *IEEE Trans. Magn.*, vol. MAG-15, no. 3, pp. 1075-1084, May 1979.
- [8] R. T. Smith, "Circuit analysis of eddy currents," *IEEE Trans. Aerosp. Electron Syst.*, vol. 11, no. 4, pp. 495-498, July 1975.
- [9] J. P. Webb, B. Forghaini, and D. A. Lowther, "An approach to the solution of three-dimensional voltage driven and multiply connected eddy current problems," *IEEE Trans. Magn.*, vol. 28, no. 2, pp. 1193-1196, March 1992.
- [10] J. Shen and A. Kost, "BEM with mixed special shape functions for 2D eddy current problems," *IEEE Trans. Magn.*, vol. 28, pp. 1220-1223, March 1992.
- [11] T. Ueyama, S. Nishi, K. Wajima, K. Umetsu, and T. Nishisaka, "3-D Analysis of electromagnetic field including conductors connected with voltage sources," *IEEE Trans. Magn.*, vol. 29, no. 2, March 1993.
- [12] T. Onuki and S. Wakao, "Novel boundary element analysis for 3D-eddy current problems," *IEEE Trans. Magn.*, vol. 29, no. 2, pp. 1520-1523, March 1993.
- [13] Z. Azzouz, A. Foggia, L. Pierrat, and G. Meunier, "3D finite element computation of the high frequency parameters of power transformer windings," *IEEE Trans. Magn.*, vol. 29, no. 2, pp. 1407-1410, March 1993.
- [14] Q. Chen, A. Konrad, and P. P. Biringer, "An integrodifferential finite element—Green's function method for the solution of unbounded eddy current problems," *IEEE Trans. Magn.*, vol. 29, no. 2, pp. 1874-1977, March 1993.
- [15] O. V. Tozoni, "Computer-aided electromagnetic field calculation," *Technika*, USSR, 1967.

I. Marinova biography not available at time of publication.

Y. Midorikawa biography not available at time of publication.

S. Hayano biography not available at time of publication.

Y. Saito biography not available at time of publication.